64-QAM LTE signal transmission at 25 GHz over hybrid SSMF and non-uniform turbulent FSO channel

Luis Vallejo
Instituto de Telecomunicaciones y Aplicaciones Multimedia
Universitat Politecnica de Valencia
Valencia, Spain
luivalc2@iteam.upv.es

Dong-Nhat Nguyen
Department of Electromagnetic Field
Czech Technical University in Prague
Prague, Czech Republic
dongnhat@fel.cvut.cz

Stanislav Zvanovec
Department of Electromagnetic Field
Czech Technical University in Prague
Prague, Czech Republic
xzvanove@fel.cvut.cz

Beatriz Ortega
Instituto de Telecomunicaciones y Aplicaciones Multimedia
Universitat Politecnica de Valencia
Valencia, Spain
bortega@dcom.upv.es

Jan Bohata
Department of Electromagnetic Field
Czech Technical University in Prague
Prague, Czech Republic
bohatja2@fel.cvut.cz

***Abstract*—This contribution describes the impact of non uniform thermal-induced turbulence on 64-QAM LTE signal transmission at 25 GHz millimeter wave (mmW) signal along hybrid RoF/RoFSO links. Microwave photonic signal generation has been employed by using the optical frequency doubling with intensity modulator biased at the minimum transmission point. The optical and electrical power budgets of different scenarios have been defined and error vector magnitude (EVM) performance has been measured. It is shown that the uniform scenario with high turbulence in the middle of the link is the one with greater impact on the quality of the received data.**

Keywords—Free space optics communications, hybrid RoF/RoFSO, thermal turbulence, millimetre-waves.

I. INTRODUCTION

Nowadays, mobile communications are inside of our daily life. In 2022, there will be 12.3 billion mobile connected devices, including machine-to-machine (M2M) modules and therefore, exceeding the world´s forecast population at that time by one and a half times. Mobile data traffic will be 77 exabytes and fourth generation (4G) connections will have more than 71 % of the total mobile traffic [1]. In order to deal with such demand, a new mobile network technology is needed, i.e., fifth generation (5G). New emerging services and applications, such as Internet of Things (IoT), massive machine to machine (mM2M), mobile ultra-high definition (UHD) video streaming or autonomous driving [2] require massive machine type communications (mMTC), ultra-reliable and low latency communications (URLLC), enhanced mobile broadband (eMBB) and ultra-fast data transfer [3].

Lower frequencies (below 6 GHz) are heavily congested with TV and radio signals, WiFi networks and also current mobile networks, i.e. second (2G), third (3G) and fourth (4G) generation. Millimeter wave (mmW) technology, which frequency range is up to 300 GHz, will play a key role in 5G networks owing to its enormous available bandwidth to provide high data transmission. However, some challenges such as mmW signal generation since traditional RF signal is generated by costly electronic stages and high attenuation (i.e. $\sim$2.5 dB/m at 25 GHz over metallic cable) must be properly addressed before massive adoption.

From that perspective, radio-over-fiber (RoF) is a promising technology to transmit mmW signals because of its advantages, such as low attenuation loss, immunity to radio frequency interference, transparency to modulation formats, high capacity, flexibility and dynamic resource allocation as its main advantages [4]. RoF consists basically of a lightwave modulated by a radio signal and transmitted over an optical link, commonly based on optical fiber (OF). Moreover, the usage of RoF in 5G cloud-RAN (C-RAN) architecture is an excellent solution for such fronthaul link, which can transport mmW signals carrying data rates of Gb/s along tens of kilometres of optical fiber (OF) [5, 6].

Microwave photonics (MWP), which is an interdisciplinary area that merges microwave and optical signals, is capable to generate mmW signals. MWP allows to generate mmW signals in the optical domain with low phase noise and frequency tunability [7]. Numerous mmW generation schemes have been demonstrated in the literature [8], from the basic heterodyne beating up to the signal generation based on non-linear effects. In particular, the external modulation approach based on optical frequency multiplication between the modulated sidebands has been demonstrated as a very convenient approach in terms of cost and complexity, which allows to achieve frequency doubling, quadrupling and up to 8-tupling [9] with significant reduction of the electric bandwidth requirements.

Free space optics (FSO) is a wireless communication system for optical signal transmission. FSO operates in the infrared spectrum, which uses extremely narrow beams in line

of sight (LOS), and can provide links with high data rate, i.e. up to hundreds of Gb/s [10]. Its main advantages are the enormous available bandwidth and no license fees are required due to the use of THz frequencies and flexibility [11]. In addition, OF infrastructure is generally expensive in urban areas and FSO is an excellent alternative where OF cannot be installed. However, FSO is very sensitive to atmospheric conditions, i.e. fog or mist, clouds, rain, snow [12]. Besides, misalignments, so-called pointing errors, due to buildings thermal expansion, wind or weak seismic activity, amongst others, must also be considered and further compensated [13, 14].

Especially, FSO is altered by atmospheric turbulence created by temperature gradients [15, 16, 17] occuring naturally in an outdoor environment. Examples of them are thermal distributions produced along an optical path either as cold (rivers, forest…) or hot (cars, buildings, smokestacks…) sources. The impact of uniform [18] and non-uniform [19] thermal turbulence has been studied along the radio-over-FSO (RoFSO) links.

In this work, we evaluate the impact of the uniform and non-uniform thermal distribution over a 64-QAM LTE signal at 25 GHz, which is photonically generated by external modulation with carried suppression (CS).

II. System Setup

The experimental system layout of 64-QAM LTE signal transmitted at 25 GHz over a hybrid standard single mode fiber (SSMF) and FSO link is shown in Fig. 1(a). In our setup, the Mach-Zehnder modulator (MZM) is biased at its half-wave voltage, V_π, to modulate the optical wavelength by a sinusoidal wave at radio frequency (f_{RF}). Provided all even-order sidebands are suppressed and the second and higher-order optical sidebands can be ignored, the modulated optical signal at the MZM output is given by [20]:

$$E_{out}(t) = E_0 \left\{ J_1\left(\pi \frac{V_{RF}}{2V_\pi}\right) \cos\left((w_c + w_{RF})t\right) + J_1\left(\pi \frac{V_{RF}}{2V_\pi}\right) \cos\left((w_c - w_{RF})t\right) \right\} \quad (1)$$

where E_0 and w_c are the amplitude and angular frequency of the optical carrier, V_{RF} is the voltage amplitude, $w_{RF} = 2\pi f_{RF}$ is the angular frequency of the sinusoidal wave and $J_1(\cdot)$ is the first-order Bessel function of the first kind. Therefore, the optical carrier is suppressed without a need for optical filters and the beating between both sidebands at the optical receiver generates the mmW signal at double the drive frequency, $f_{mmW} = 2f_{RF}$.

In this architecture, the laser emits an optical lightwave with 16 dBm output power at 1550.496 nm, whose state of polarization is adjusted by the polarization controller (PC) at the optical input of the modulator (MZM-1). The MZM-1 (Fujitsu FTM7938EZ/201) is biased at null transmission point, i.e. 2.86 V, to suppress the optical carrier, and modulated with a RF single-tone signal having power of 22 dBm at 12.5 GHz, which is generated by a signal generator (SG) (R&S SMF100A). The signal is further modulated by data in the MZM-2 (Covega 10TM 081), which is biased at the quadrature point (1.83 V). Data of 20 MHz bandwidth 64-QAM signal are generated with 9 dBm output power by a vector signal generator (VSG) (R&S SMW200A) using an intermediate frequency of 200 MHz . An EDFA with 13.2 dBm constant output power is employed to compensate optical losses. The hybrid link is formed with 5 km SSMF and 2 m FSO link. Then, the optical signal is launched into the photodetector (OptiLab PD-40). Finally, the electrical signal, generated by beating in photodetector at 25 GHz is analysed by a RF spectrum analyzer (RFSA) (R&S FSW26).

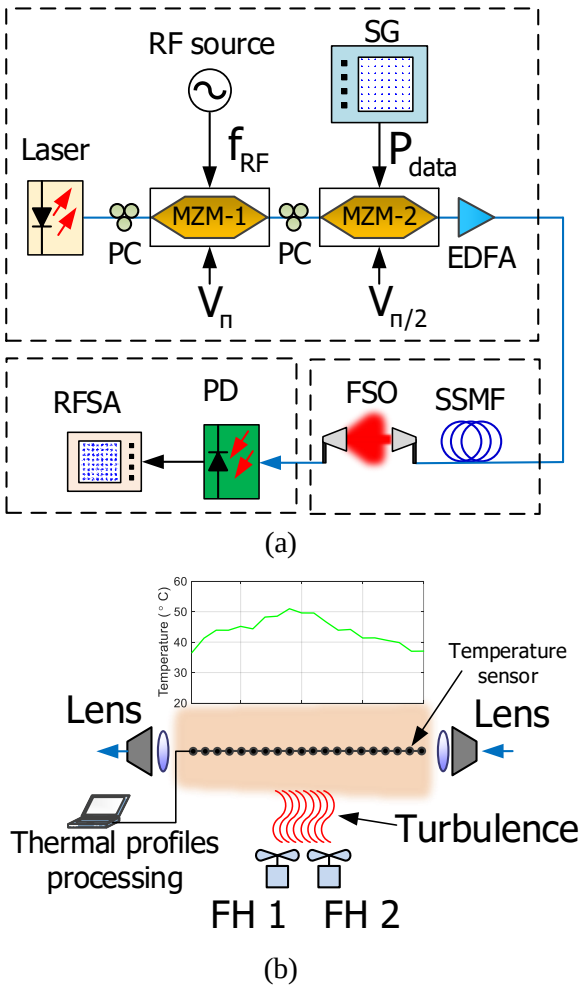

Figure 1. (a) System layout, (b) Scheme of FSO turbulence generation. PC: polarization controller, MZM: Mach-Zehnder modulator, SG: signal generator, EDFA: erbium doped fiber amplifier, SSMF: standard single mode fiber, FSO: free space optics, PD: photodetector, RFSA: RF spectrum analyser, FH : fan heater.

The FSO link uses a pair of air-spaced doublet collimators (Thorlabs 114 F810APC-1550) with 4 dB optical loss in the wireless segment. Two fan heaters (FH) are employed to generate thermal turbulence, as depicts Fig. 1(b). Then, the temperature gradient is measured by 20 temperature sensors equidistantly separated (0.1 m) and processed on a computer.

Temperature and structure refractive index distributions (C_n^2) are shown in Fig. 2. C_n^2 is calculated based on Gamma-Gamma model [21] using the recorded temperature gradient, sensor gap and the atmospheric pressure. Temperature and structure refractive index distributions [21] are shown in Fig. 2. D1 represents a turbulence distribution with increased turbulence level at the receiver side, D2 shows an increased turbulence level at the transmitter side, and D3 with an increased turbulence level in the middle of the link.

Tab. 1 shows the calculated refractive index and Rytov variance [21] from measured thermal distributions.

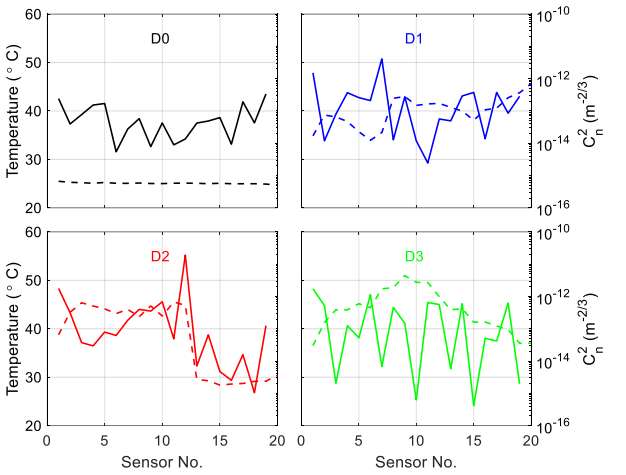

Figure 2. Temperature (dashed line) and C_n^2 (solid line) for different temperature distributions.

Table 1. C_n^2 and Rytov variance for thermal distributions

Scenario	$C_n^2(m^{-2/3})$	Rytov variance
D0	$8.3 \cdot 10^{-14}$	$1.86 \cdot 10^{-5}$
D1	$4.4 \cdot 10^{-13}$	$9.90 \cdot 10^{-5}$
D2	$1.2 \cdot 10^{-12}$	$2.75 \cdot 10^{-4}$
D3	$3.5 \cdot 10^{-13}$	$7.95 \cdot 10^{-5}$

III. Results

A. Millimeter wave signal generation

Fig. 3(a) shows the optical spectra of the transmitted signal over scenarios with different turbulence distributions, as described in Fig. 2. The impact of the thermal-induced turbulence is an optical power reduction of 2, 0.16 and 8 dB for D1, D2 and D3 respect to D0, respectively.

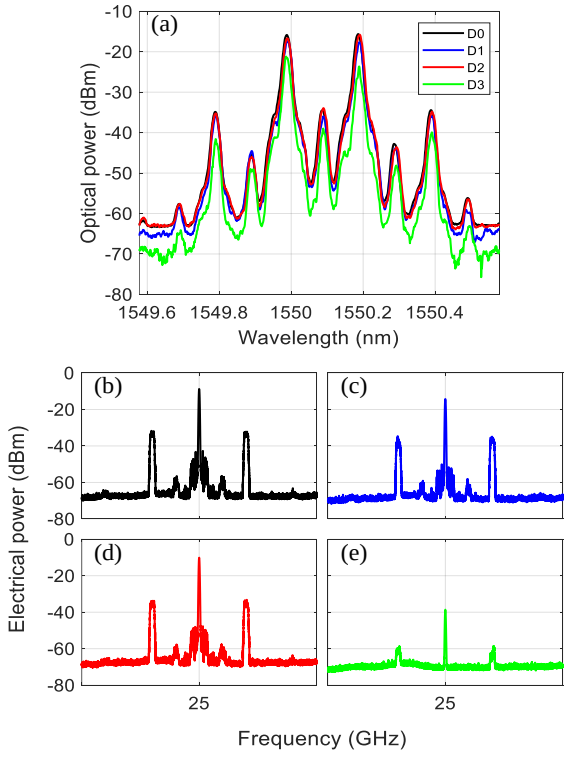

Figure 3. (a) Optical spectra before detection of the signal transmitted over different scenarios, and (b)-(e) Electrical spectra of the received signal after transmission over D0-D3 scenarios (1 GHz span) with 6 dBm optical power at the PD input.

After opto-electronic conversion, the electrical signal was measured by an RF spectrum analyser (RFSA) in order to evaluate the impact of the thermal turbulences in terms of the RF power. Fig. 3(b)-(e) show the electrical spectrum for D0-D3. As can be seen, RF power decrease follows the optical power, where the data band shows a power decrease due to the turbulence levels.

Fig. 4 shows the received optical and electrical power values for particular scenarios D0-D3 in order to show the power budget for different scenarios. In our setup, when the optical power is set at D0 as -15.62 dBm, less than 2 dB optical power decrease is measured for D1-D2 but up to 8 dB reduction is obtained when the turbulence D3 is applied in the FSO link. In this case, the measured RF power at 25 GHz is -8.77 dBm for D0, and up to 29.85 dB power decrease is obtained when the turbulence D3 is applied in the FSO link.

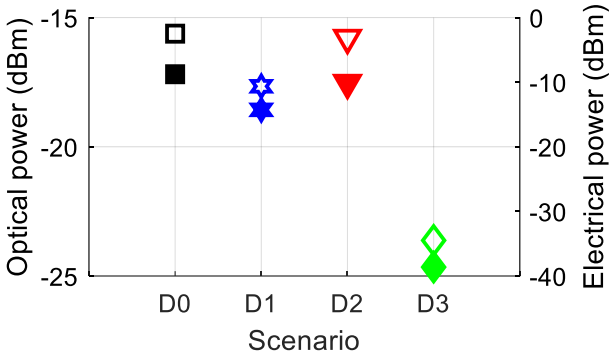

Figure 4. Optical (empty markers) and electrical (filled markers) power.

B. Data transmission

In this section, we evaluated the effect of the turbulence on the quality of the data signal transmitted along the proposed hybrid link. The 25 GHz mmW optical signal is modulated with 64-QAM signal with 20 MHz bandwidth at intermediate frequency of 200 MHz. It results in a bitrate of 75 Mb/s throughout the hybrid link.

Fig. 5 shows the measured constellations of recovered signals after detection when the received optical power is 0 dBm. The larger degradation is measured in D3 scenario, which corresponds to the worst power budget in Fig. 4, and therefore, the lower electrical power level.

Finally, Fig. 6 plots error vector magnitude (EVM) versus the received optical power for all measured scenarios. Tab. 2 summarizes the minimum received optical power, i.e. sensitivity of the links for satisfying the 8 % EVM standard threshold level for 64-QAM [22]. There is no significant penalty between D0 and D2 meanwhile the penalty between D0 and D1 is 3.6 dB. The largest measured EVM values correspond to D3, where the power penalty between weak turbulence and strong turbulence regime with maximum level in the middle of the link is 6.5 dB.

Table 2. Sensitivity (8 % EVM level).

Distribution	Optical power (dBm)
D0	-7.83
D1	-4.27
D2	-6.96
D3	-1.3

Fig. 7 shows the equivalent bit error rate (BER) [23] and the BER limit using forward error correction (FEC) [24]. It is shown that the largest BER is measured in D3 meanwhile there are almost no differences between D0 and D2.

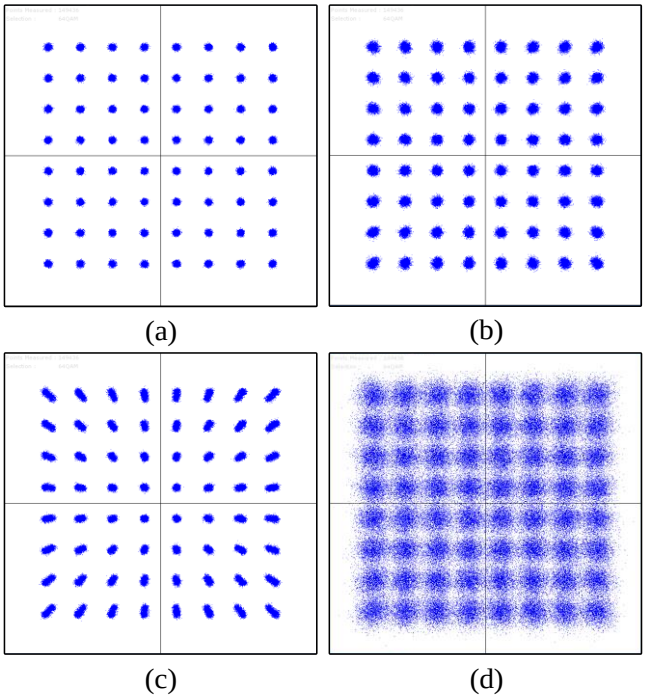

Figure 5. Constellations for (a) D0, (b) D1, (c) D2 and (d) D3 with 0 dBm at the PD input.

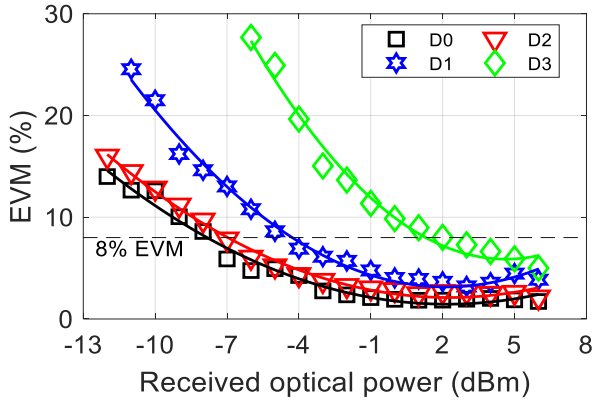

Figure 6. EVM measurements for different scenarios vs received optical power.

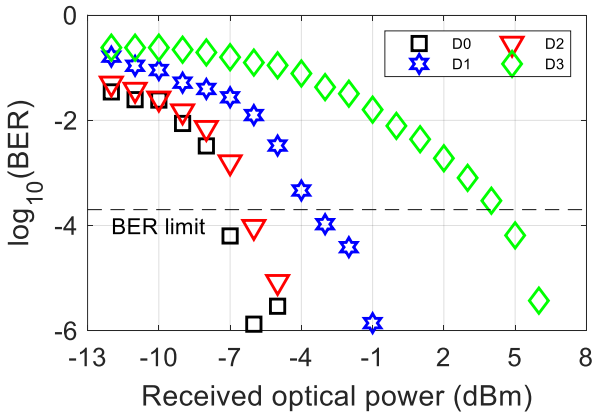

Figure 7. Calculated BER for different scenarios vs received optical power.

IV. Conclusions

In this work, we experimentally demonstrated the impact of the thermal turbulence with different distribution on the 64-QAM LTE signal at 24 GHz mmW signal along hybrid RoF/RoFSO links. The mmW signal has been photonically generated by employing optical frequency doubling in a CS modulated signal. The power budget of the system leads to an optical and electrical power decrease up to 8 dB and 29.85 dB, respectively, which have been recorded in the strongest turbulent scenario. The EVM degradation of 20 MHz 64-QAM signal confirms that the non-uniform scenario with high turbulence in the middle of the link has significant impact on the quality of the received data.

Acknowledgment

This work was also supported by the Research Excellence Award Programme GVA PROMETEO 2017/103, the Spanish Ministerio de Ciencia, Innovación y Universidades RTI2018-101658-B-I00 FOCAL project, Ministry of Industry and Trade in Czech Republic project (FV30427) and within COST CA16220.

References

[1] "Cisco Visual Networking Index: Forecast and Trends, 2017-2022," Cisco, Feb 2019.

[2] R. Waterhouse and D. Novack, "Realizing 5G: microwave photonics for 5G mobile wireless systems," IEEE Microwave Magazine, vol. 16, no. 8, pp. 84-92, Sept. 2015.

[3] ETSI, "TR 38.913 V 15.0.0. 5G; Study on scenarios and requirements," 2018.

[4] C. H. Lee, Microwave Photonic, 2nd ed., Taylor & Francis, 2013.

[5] C. Lim, Y. Tian, C. Ranaweera, T. Ampalavanapillai Nirmalathas, E. Wong and K.-L. Lee, "Evolution of Radio-Over-Fiber Technology," Journal of Lightwave Technology, vol. 37, no. 6, pp. 1647-1656, 2019.

[6] A. Checko, H. L. Christiansen, Y. Yan, L. Scolari, G. Kardaras, M. S. Berger and L. Dittmann, "Cloud RAN for mobile networks - A technology overview," IEEE Communications Surveys & Tutorials, vol. 17, no. 1, pp. 405-426, 2015.

[7] Y. Doi, S. Fukushima, T. Ohno and K. Yoshino, "Frequency stabilization of millimeter-wave subcarrier using laser heterodyne source and optical delay line," IEEE Photonics Technology Letters, vol. 13, no. 9, pp. 1002-1004, September 2001.

[8] J. Yao, "Microwave photonics," Journal of Lightwave Technology, vol. 27, no. 3, pp. 314-335, February 2009.

[9] H. Zhang, L. Cai, S. Xie, K. Zhang, X. Wu and Z. Dong, "A novel radio-over-fiber system based on carrier suppressed frequency eightfold millimeter wave generation," IEEE Photonics Journal , vol. 9, no. 5, 2017.

[10] Z. Zhao, Z. Zhang, J. Tan, Y. Liu and J. Liu, "200 Gb/s FSO WDM communication system empowered by multiwavelength directly modulated TOSA for 5G wireless networks," IEEE Photonics Journal, vol. 10, no. 4, 2018.

[11] M. A. Khalighi and M. Uysal, "Survey on free space optical communication: a communication theory perspective," IEEE Communications Surveys & Tutorials, vol. 16, no. 4, pp. 2231-2258, January Forthquarer 2014.

[12] Z. Ghassemlooy, W. Popoola and S. Rajbhandari, Optical wireless communications. System and channel modelling with Matlab, 2nd ed., CRC Press Taylor & Francis group, 2019.

[13] D. K. Borah and D. G. Voelz, "Pointing Error Effects on free-space optical communication links in the presence of atmospheric turbulence," Journal of Lightwave Technology, vol. 27, no. 18, pp. 3965-3973, September 2009.

[14] M. A. Esmail, A. Ragheb, H. Fathallah and M.-S. Alouini, "Investigation and demonstration of high speed full-optical hybrid FSO/fiber communication system under light sand storm condition," IEEE Photonics Journal, vol. 9, no. 1, pp. 1-12, 2017.

[15] J. Libich and S. Zvanovec, “Influences of turbulences in near vicinity of buildings on free-space optical links,” IET Microwaves, Antennas & Propagation, vol. 5, no. 9, pp. 1039-1044, June 2011.

[16] K. Niachou, I. Livada and M. Santamouris, “Experimental study of temperature and airflow distribution inside an urban street canyon during hot summer weather conditions. Part II: Airflow analysis,” Building and Environment, vol. 43, no. 8, pp. 1393-1403, August 2008.

[17] D.-N. Nguyen, J. Bohata, J. Spacil, D. Dousek, M. Komanec, S. Zvanovec, Z. Ghassemlooy and B. Ortega, “M-QAM transmission over hybrid microwave photonic links at the K-band,” Optics Express, vol. 27, no. 23, pp. 33745-33756, 2019.

[18] D.-N. Nguyen, J. Bohata, M. Komanec, S. Zvanovec, B. Ortega and Z. Ghassemlooy, “Seamless 25 GHz transmission of LTE 4/16/64-QAM signals over hybrid SMF/FSO and wireless link,” Journal of Lightwave Technology, vol. 37, no. 24, pp. 6040-6047, 2019.

[19] L. Vallejo, M. Komanec, B. Ortega, J. Bohata, D.-N. Nguyen, S. Zvanovec and V. Almenar, “Impact of thermal-induced turbulent distribution along FSO link on transmission of photonically generated mmW signals in the frequency range 26–40 GHz,” IEEE Photonics Journal, vol. 12, no. 1, 2020.

[20] C.-T. Lin, J. Chen, S.-P. Dai, P.-C. Peng and S. Chi, "Impact of nonlinear transfer function and imperfect splitting ratio of MZM on optical up-conversion employing double sideband with carrier suppression modulation," Journal of Lightwave Technology, vol. 26, no. 15, pp. 2449-2459, 2008.

[21] L. C. Andrews and R. L. Phillips, Laser Beam Propagation through Random Media, 2nd ed., SPIE Press, 2005.

[22] ETSI, “TS 138.101-2 V15.7.0. User Equipment (UE) radio transmission and reception; Part 2: Range 2 Standalone,” 2019.

[23] X. Chen and J. Yao, “A high spectral efficiency coherent microwavephotonic link employing both amplitude and phasemodulation with digital phase noise cancellation,” Journal of Lightwave Technology, vol. 33, no. 14, pp. 3091-3097, 2015.

[24] C. B. Naila, K. Wakamori, M. Matsumoto, A. Bekkali and K. Tsukamoto, “Transmission analysis of digital TV signals over a Radio-on-FSO channel,” IEEE Communications Magazine, vol. 50, no. 8, pp. 137-144, 2012.